Journal of Russian Laser Research, Volume 31, Number 5, 2010

THERMOELECTRIC PROPERTIES OF TUNNEL JUNCTIONS

Igor E. Protsenko

P. N. Lebedev Physical Institute, Russian Academy of Sciences
Leninskii Prospect 53, Moscow 119991, Russia
Plasmonics Ltd, Niznie Polya Street 29/1, Moscow 109382, Russia
E-mail: protsenk @ gmail.com

Abstract

The thermoelectric (Seebeck) coefficient α and thermoelectric quality factor (figure of merit) ZT are estimated for a tunnel junction in metals. It is shown that α can be of the order of hundreds of μV/K while ZT can approach values $\sim$0.1–1. The maxima of $\alpha(h)$ and $ZT(h)$ correspond to a certain width h of the tunnel junction; such h is about a few nanometers. The results we obtained can find applications in the constructions of novel thermoelectric generators.

Keywords: thermoelectric convertor, tunnel junction, figure of merit.

1. Introduction

The thermoelectric generator (TEG) is a device for direct transformation of heat energy to electricity with the help of thermoelectric materials (thermoelectrics). An ideal TEG has many advantages versus other electric sources — long operating life and long period of storage, quick switch on and off any time, no technical support necessary. TEGs provide a stable voltage and do not suffer from shortcut and free running regimes. They work without any noise since they do not contain moving parts, which is an advantage in comparison with machine sources of constant voltage. Thus, TEGs can be used in areas that require super-reliable sources of electricity with long-term service without technical support, as in automatic weather stations, sea beacons, and space satellites.

The first widely used TEGs were built by the group of Prof. A. F. Ioffe — the well-known "Guerrilla Kettle" based on metal thermoelectric elements from SbZn and a copper–nickel alloy (constantan) with 55% of copper and 45% of nickel. A temperature difference of 250–300° was provided by the flame at the hot SbZn–constantan connections and temperature stabilization at cold connections by boiling water. This device, in spite of a low energy-conversion-efficiency (ECE factor) of 1.5–2.0%, was successfully used as an energy supply for portable radio stations [1].

At present, metallic TEGs are exclusively employed for temperature measurements [2] due to their low efficiency. Semiconductor materials are usually used for generation of electricity; very often such materials are solid solutions of chalcogenides of elements of V and IV groups and solid solutions of Si–Ge. Semiconductors are preferred because of their high thermo-EMF coefficient – of the order of hundreds of μV/deg, which is one order of magnitude greater than thermo-EMF coefficients of metals.

Manuscript submitted by the author in English on September 6, 2010.
1071-2836/10/3105-0481

However, semiconductor TEGs are not as reliable as metallic TEGs. Operation of semiconductor TEGs at high temperatures requires special anticorrosion and antisublimation protection of thermoelements and insertions of protective layers for reducing chemical interaction of semiconductor materials with electric connectors with matching thermal expansion between all layers. Such and other layers shunt the thermal flux and build an additional thermal resistance, which leads to a reduction in the ECE factor.

The ECEs of the best semiconductor TEG reaches 15% [3]; however, the ECE of commercial semiconductor TEGs usually stays near 3–5% [1], which is only 2–2.5 times more than the ECE of metallic TEGs constructed in the 40s of the last century by Prof. A. F. Ioffe and coworkers. A low ECE factor restricts the application of TEGs, mainly, for "household needs" when the output power of TEGs does not exceed dozens of watts. One can easily observe this by analyzing, for example, offers in the Internet.

One can conclude, therefore, that at present there is no thermoelectric materials whose properties fully satisfy industry; searching for such a material is still a topical subject. Theoretical efforts in such a search are not yet successful and not quite sufficient possibly because of the complicated nature and multiple physical processes taking place in thermoelectric materials. The main tool for the search for novel thermoelectric materials is at present an experiment.

One can formulate the basic requirements for good thermoelectric materials.

1. High thermo-EMF coefficient, not less than hundreds of μV/deg, i.e., such as those required for semiconductor thermoelements or higher;

2. Low lattice thermoconductivity;

3. Low electric resistivity;

4. Reliability under harse working conditions (high temperatures, contacts with aggressive media, etc.);

5. Low cost.

Requirements 2 and 3 can be better satisfied, the lower the phonon thermoconductivity of the materials of thermoelement and the higher the carrier mobility [4]. It is considered that solid solutions of semiconductor complexes are good thermoelectric materials because of the scattering of phonons on the disordered grains, which reduces thermal oscillations of the crystalline lattice. Due to this, the phonon part of the thermal conductivity of solid solutions, for example, of Pb chalcogenides, is reduced with respect to the electron part of the thermal conductivity [5].

The search for proper thermoelectric materials is still in progress. It was suggested to use the thermo-EMF in the presence of potential barriers with nonequilibrium carrier current in semiconductors [6]. In [7] was shown that the thermoelectric quality factor (figure of merit) for such systems is close to that in the best thermoelectric materials.

In this paper, we study a thermoelement on the tunnel junction. It is shown that under certain conditions the thermo-EMF coefficient of such a junction is quite high. As a consequence, such a TEG has a large figure of merit — of the order of that for semiconductor thermoelements or even greater. Thus, it is attractive to investigate materials with tunnel junctions as potential candidates for thermoelectric materials, in particular, metals. Such a TEG preserves the advantages of well-known metallic TEGs, such as the reliability under harsh working conditions. It is well understood, however, that there are many problems to be solved before approaching a high ECE factor of metallic TEGs with tunnel junctions,

as was mentioned also in [8], where thermoelectric phenomena in a cluster of metal nanoparticles were studied.

A brief review of the theory of TEGs is given in the following section and the expression for the ECE factor of a thermocouple is derived following [10] (with a small variation). The characteristics of metallic and semiconductor thermocouples are estimated and compared with each other in Sec. 3. The thermo-EMF coefficient of a tunnel junction with metal banks and the figure of merit are calculated in Sec. 4. Results are discussed in Sec. 5.

2. Expression for the Thermocouple ECE Factor

The energy conversion efficiency (ECE factor) of a thermocouple is

$$\eta = \frac{W_R}{W_R + W_r}, \tag{1}$$

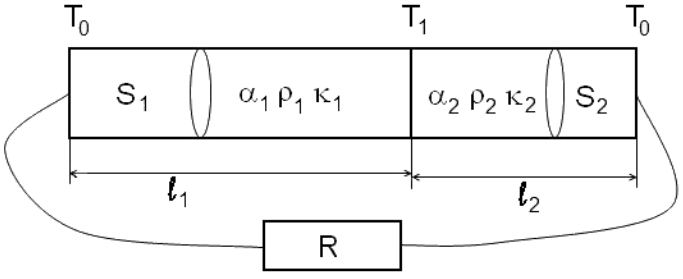

Fig. 1. Scheme of a thermocouple. T_1 is the temperature of the hot connection of materials 1 and 2 (thermoelements), and T_0 is the temperature of the cold connection.

where W_R is the power extracted on the load, W_r is the power extracted by the thermocouple, $W_R + W_r$ is the total power extracted in the circuit, which contains the load with resistance R and the thermocouple with resistance $r = (\varrho_1 l_1/S_1) + (\varrho_2 l_2/S_2)$, and S_i, l_i, and ϱ_i are, respectively, the cross-sectional areas, lengths, and specific resistances of elements of the thermocouple made of metals ($i = 1, 2$); see Fig. 1.

If I is the current in the circuit, then $W_R = I^2 R$ and

$$W_r = K(T_1 - T_0) + Q_T + Q_P. \tag{2}$$

Here the first term is the power of the thermal flux lost by the thermocouple due to thermoconductivity to the environment. It is assumed that the temperature T of the thermocouple with length l and cross-sectional area S varies linearly with the coordinate z along the thermocouple starting from T_1 at the hot end and approaching T_0 at the cold end, so that

$$T(z) = (T_0 - T_1)(z/l_i) + T_1. \tag{3}$$

The thermal flux moves from the hot end through cross-sections of the thermoelements so that $K = (\varkappa_1 S_1/l_1) + (\varkappa_2 S_2/l_2)$, where $\varkappa_{1,2}$ are specific heat conduction coefficients. The terms Q_T and Q_P in (2) are, respectively, the Thomson and Peltier heats. Expression (2) does not include the Joule heat $I^2 r$ extracted at the thermocouple because half of such heat is extracted on the hot end and gives a positive contribution to the thermo-EMF, while the other half is extracted on the cold end removing the thermal energy from the thermocouple. Thus, such a Joule heat does not change the thermocouple energy. Expressions (1) and (2) differ from the expression of [10] by an extra term W_R in the denominator of (1), so that estimates of η made with the help of (1) and (2) are lower than ones obtained in [10].

The electric field arising in the material due to the temperature gradient is $E_T = \alpha(dT/dz)$, where α is the Seebeck (proportionality) coefficient or the thermo-EMF coefficient. The thermo-EMF is

$$\mathcal{E}_T = \left| \int_0^l \alpha(dT/dz)\, dz \right| = |\alpha_1 - \alpha_2|\,(T_1 - T_0), \tag{4}$$

in the approach where α_i of both materials $i = 1, 2$ does not depend on temperature. Since the thermoelectric current must cause rebuilding of thermal equilibrium between the cold and hot ends of the thermocouple, the Peltier heat (as well as the heat flux due to thermoconductivity) moves out of the hot junction of the materials of the thermocouple. According to [11],

$$Q_P = IT_1|\alpha_1 - \alpha_2|. \tag{5}$$

On the assumption that α_i does not depend on temperature, the Thomson heat $Q_T = 0$, so that

$$\eta = \frac{I^2R}{I^2R + K\Delta T + IT_1\Delta\alpha}, \qquad \Delta T = T_1 - T_0, \qquad \Delta\alpha = |\alpha_1 - \alpha_2|. \tag{6}$$

Inserting $I = \mathcal{E}_T/(R + r) = \Delta\alpha\Delta T/(R + r)$ in Eq. (6) and denoting $m \equiv R/r$, we obtain

$$\eta = \frac{\Delta T}{T_1} \frac{\dfrac{m}{m+1}}{1 + \dfrac{\Delta T}{T_1}\dfrac{m}{m+1} + \dfrac{Kr(1+m)}{\Delta\alpha^2 T_1}}. \tag{7}$$

Expression (7) can be converted to formula (5) from [10] (p. 274) if one removes the term $\sim \Delta T/T_1$ from the denominator of Eq. (7); this term is responsible for the losses caused by the Joule heat released on the load of the thermocouple. Denoting the thermodynamic ECE factor as $\eta_T = \Delta T/T_1$ and introducing the thermoelectric quality factor (figure of merit)

$$Z = \Delta\alpha^2/(Kr), \tag{8}$$

one can rewrite Eq. (7) as follows:

$$\eta = \eta_T \frac{m}{1 + m(1 + \eta_T) + (1 + m)^2/(ZT_1)}. \tag{9}$$

After taking the derivative of Eq. (9) with respect to m, we obtain that η has a maximum at $m = m_0$, where

$$m_0 = [1 + ZT_1]^{1/2}. \tag{10}$$

Inserting Eq. (10) into Eq. (9), we obtain the maximum of the thermocouple ECE factor for given ZT_1 and η_T

$$\eta_{\max} = \frac{\eta_T}{1 + \eta_T + 2(1 + m_0)/(ZT_1)} = \frac{\eta_T}{1 + \eta_T + (ZT_1/2)[1 + (1 + ZT_1)^{1/2}]}. \tag{11}$$

From Eq. (11), one can see that the thermocouple ECE factor has an absolute maximum at $ZT_1 \gg 1$ (and at $m_0 \gg 1$). This maximum is $\eta_{\mathrm{MAX}} = \eta_T/(1 + \eta_T) < \eta_T$.

Examining the structure of Eq. (11), one can see two principal tasks in the construction of thermoelectric devices.

Task I is to find a thermoelectric material with the highest possible figure of merit ZT, and task II is to provide the maximum possible drop of temperature ΔT along the thermoelectric material in order

to reach the highest possible ΔT and, therefore, an ECE factor of an ideal heat machine η_T is close to unity. Task II is connected more with TEG engineering construction, while task I concerns the physical properties of thermoelectric materials. Successful solution of both tasks leads to a high ECE factor of thermoelectric devices. Here we are looking for a material with a high figure of merit and save the problem of providing a high ΔT for the future.

Before considering thermoelectric materials with tunnel junctions, we provide a brief comparison of metal and semiconductor thermoelectrics in the following section.

3. Estimate of the Thermocouple ECE Factor

3.1. Application of the Wiedemann–Franz Law

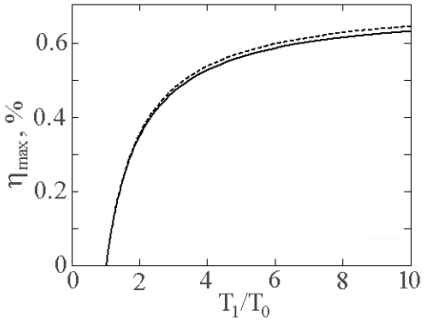

Fig. 2. Maximum ECE factor for a Fe–constantan thermocouple.

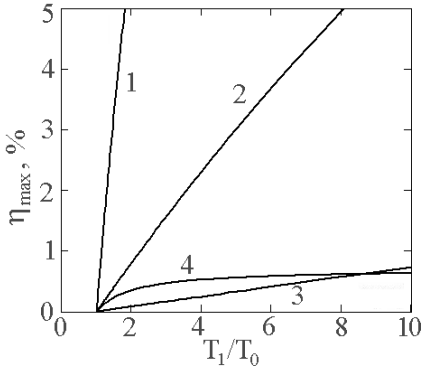

Fig. 3. Maximum ECE factor for a thermocouple with a semiconductor ($\alpha = 150$ μV/K and $\varkappa = 0.02$ W/K·cm). Partial resistances of a semiconductor with $\varrho = 10^{-3}$ Ω·cm (curve 1), 10^{-2} Ω·cm (curve 2), and 10^{-1} Ω·cm (curve 3), and of a Fe–constantan thermocouple (curve 4).

One can estimate the heat conduction coefficient of metals with the help of the Wiedemann–Franz law [12]

$$\varkappa_i \varrho_i = LT, \tag{12}$$

where $L = 3.28\,(k_B/e)^2 T = 2.445 \cdot 10^{-8}$ W·Ω/K^2 is the Lorentz number, k_B is the Boltzmann constant, and e is the electron charge.

Assuming that Eq. (12) is valid for metals, one can see that Kr in the figure of merit given by Eq. (8) has a maximum at $\varrho_2 S_1 L_2/(\varrho_1 S_2 L_1) = \varrho_1 S_2 L_1/(\varrho_2 S_1 L_2)$. Assuming that the last relation is satisfied, we obtain

$$ZT_1 = \Delta\alpha^2/(4L). \tag{13}$$

Let us consider, for definiteness, a Fe–constantan thermocouple. For Fe, $\alpha_{\text{Fe}} = +15$ μV/K, and for constantan $\alpha_{\text{const}} = -38$ μV/K (with respect to Pl, see [13]). Thus $\Delta\alpha = 15 - (-38) = 53$ μV/K, so that $ZT_1 = 0.03 \ll 1$.

Figure 2 shows the dependences $\eta_{\max}(T_1/T_0)$ obtained in view of Eq. (11) (solid curve) and with the help of an approximate relation

$$\eta_{\max} \approx \eta_T ZT_1/4 \tag{14}$$

(dashed curve), which is good approximation for Eq. (11) at $ZT_1 \ll 1$. We take $\alpha = 150$ μV/K and $\varkappa = 0.02$ W/K·cm, following [10] (p. 308), and take three values of partial resistance $\varrho = 10^{-3}$, 10^{-2}, 10^{-1} Ω·cm (curves 1–3 in Fig. 3). As for curve 4 in Fig. 3, it is the same as in Fig. 2 for the case $Z = (\alpha)^2/\varkappa\varrho$ and $T_0 = 300$ K. From Fig. 3, one can see that the ECE factor of semiconductor thermoelements is greater than that of metal ones for specific resistances of semiconductors less than 10^{-1} Ω·cm. For example, for doping with Si of n (p) type, $\varrho < 10^{-1}$ Ω·cm at concentrations n_d (n_a) of donor (acceptor) impurities $n_d > 10^{17}$ cm^{-3} ($n_a > 7 \cdot 10^{17}$ cm^{-3}) at $T = 300$ K [14] (p. 465), ϱ decreases with temperature.

3.2. Application of the Experimental Data for Heat and Electrical Conductances

It is well known that the Wiedemann–Franz law is valid at high and very low temperatures for most of metals [14] (p. 339), i.e., estimates of the ECE factor of metal thermocouples performed in view of the Wiedemann-Franz law are approximate.

Let us make the same estimates using the experimental data for the heat and electrical conductances of metals.

The heat conductance $\varkappa_{\rm Fe}$ of iron (ARMCO iron) at various temperatures is given in Table 1; see [14] (p. 348).

Table 1. Heat Conductance $\varkappa_{\rm const}$ of Constantan at Various Temperatures.[a]

T, K	273	473	573	673
$\varkappa_{\rm const}$, W/(m·K)	21	26	31	37

[a] see [14] (p. 351).

Table 2. Heat Conductance $\varkappa_{\rm Fe}$ of Iron (ARMCO Iron) at Various Temperatures.[b]

T, K	300	600	1000	1183
$\varkappa_{Fe}$, W/(m·K)	71	52	32	32

[b] see [14] (p. 348).

The dependences of the heat conductance on the temperature found with the help of data from Tables 1 and 2 (dots) and their polynomial approximations (solid lines) are shown in Fig. 4.

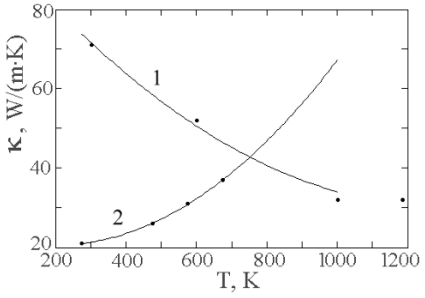

Fig. 4. Dependences of the heat conduction of Fe (1) and constantan (2) on temperature. Experimental data (dots) and their polynomial approximation using Eq. (15) (solid lines).

The heat conductance $\varkappa_{\rm const}$ of constantan and $\varkappa_{\rm Fe}$ of iron (ARMCO iron) are

$$\begin{aligned} \varkappa_{\rm const}(T) &= 23.374 - 0.029\,T + 7.273\cdot 10^{-5}\,T^2, \\ \varkappa_{\rm Fe}(T) &= 100.048 - 0.107\,T + 4.134\cdot 10^{-5}\,T^2. \end{aligned} \qquad (15)$$

If the temperature is not too low (greater than or of the order of the Debye temperature), the specific resistance $\varrho(T)$ of metals can be approximated by a linear function of temperature,

$$\varrho(T) = \varrho_0[1 + \alpha_0(T - T_0)], \qquad (16)$$

where $T_0 = 273$ K, $\varrho_0 = 8.6\cdot 10^{-6}$ Ω·cm, $\alpha_0 = 651\cdot 10^{-5}$ K^{-1} for Fe (see [14], p. 438), and $T_0 = 293$ K, $\varrho_0 = 50\cdot 10^{-6}$ Ω·cm, $\alpha_0 = -3\cdot 10^{-5}$ K^{-1} for constantan (see [14], p. 444).

Dependences (16) for Fe and constantan are shown in Fig. 5, while Fig. 6 presents the factor $\varkappa\varrho/(LT)$ obtained with the help of experimental data (Figs. 4 and 5, dots) and data interpolations (Figs. 4 and 5, solid lines). The factor $\varkappa\varrho/(LT)$ is equal to unity if the Wiedemann-Franz law is valid. One can see that the deviation $\varkappa\varrho/(LT)$ from unity does not exceed two times.

The thermodynamic Q-factor $Z = \Delta\alpha^2/(Kr)$ is maximum at

$$Kr = \left(\frac{\varkappa_{\rm Fe}S_{\rm Fe}}{l_{\rm Fe}} + \frac{\varkappa_{\rm const}S_{\rm const}}{l_{\rm const}}\right)\left(\frac{\varrho_{\rm Fe}l_{\rm Fe}}{S_{\rm Fe}} + \frac{\varrho_{\rm const}l_{\rm const}}{S_{\rm const}}\right),$$

where S and l are, respectively, the cross-sectional area and the lengths of the thermocouple metals (see Fig. 1). The maximum $Kr = [(\varkappa_{\rm Fe}\varrho_{\rm Fe})^{1/2} + (\varkappa_{\rm const}\varrho_{\rm const})^{1/2}]^2$ is reached at $[l_{\rm const}/l_{\rm Fe})(S_{\rm Fe}/S_{\rm const})]^2 =$

$\varkappa_{\text{const}}\varrho_{\text{Fe}}/(\varkappa_{\text{Fe}}\varrho_{\text{const}})$. If one assumes that the last relation is true, then Fig. 7 shows the maximum figure of merit ZT for heat conductances and specific resistances determined either from the experimental data or using the Wiedemann-Franz law.

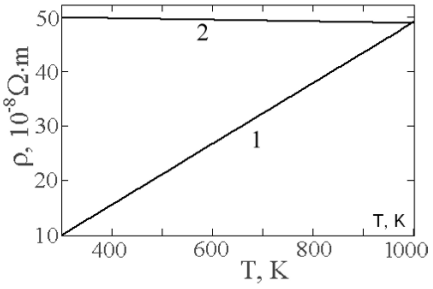

Fig. 5. Temperature dependences of specific resistances for Fe (1) and constantan (2).

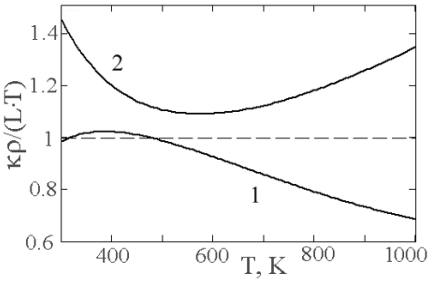

Fig. 6. Factor $\varkappa\varrho/(LT)$ for Fe (1) and constantan (2).

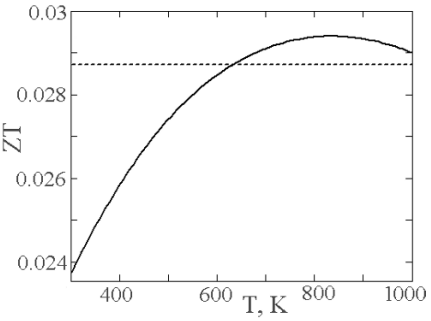

Fig. 7. Maximum figure of merit ZT found using the experimental data for $\varkappa$ and ϱ for Fe and constantan (solid curve) and in view of the Wiedemann–Franz law (dashed curve).

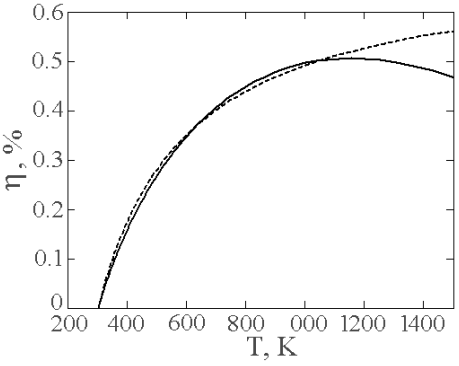

Fig. 8. Maximum ECE factor for a Fe–constantan thermocouple calculated using the experimental data for coefficients of heat conduction and specific resistance (solid curve) and in view of the Wiedemann-Franz law (dashed curve).

Figure 8 shows the maximum ECE factor of a Fe–constantan thermocouple for the heat conduction and specific resistance found from the experimental data (solid curve) and in view of the Wiedemann-Franz law (dashed curve). One can see that the results obtained in both cases are quite close to each other, except at high temperatures $T > 1200$ K.

One can see that the thermo-EMC coefficient α is a one order of magnitude greater for metals than for semiconductors, but the product $\varkappa\varrho$ is of the same order or less. Therefore, the figure of merit $Z = \alpha^2/(\varkappa\varrho)$ is one to two orders of magnitude greater for semiconductors than for metals. This is the reason for the higher ECE factor for semiconductor thermoelements than for metal ones. Since $ZT \sim \alpha^2$, it is worth looking for metal thermoelements with high α.

4. TEGs with Tunnel Junctions

From the discussion presented in the previous sections, one can conclude that the coefficient α of metal thermo-EMFs is small, about tens of μV/K, which restricts the EMC factor of metal thermocouples by values of the order of 1% or less. Otherwise, the α of semiconductor materials is usually one order of magnitude greater than that of metals; this is why the ECE factor of semiconductor thermocouples may theoretically reach 10–20%. The difference in α for metals and semiconductors is related to degeneracy of states of conduction electrons in metals and nondegeneracy of such states in semiconductors (for not too heavily doped semiconductors). The heat conduction in metals is carried out by fluxes of "hot" (fast) and

"cold" (slow) electrons with approximately equal amounts of hot and cold electrons in the total flux of carriers. The carrier concentration in semiconductors depends strongly (exponentially) on temperature, so that one can expect a greater difference in the carrier numbers in "hot" and "cold" carrier fluxes in semiconductors than in metals. Of course, if the number of free carriers is too small, the thermal current is weak anyway; so there exists an optimum free-carrier concentration with the maximum thermal power of the TEG. The other advantage of semiconductors with respect to metals consists in the fact that there are two kinds of free carriers (electrons and holes) participating in the thermal flux in semiconductors, and only one kind (electrons) in metals.

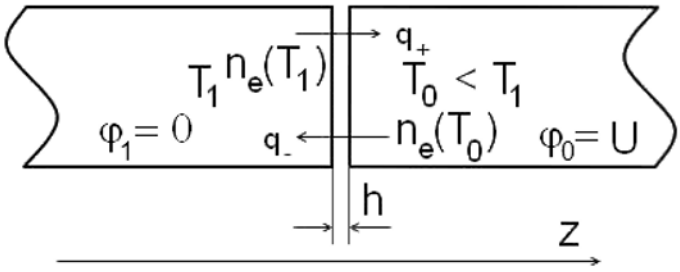

Fig. 9. Two metal conductors connected through a tunnel junction, where n_e is concentration of electrons. The higher the conductor temperature T, the larger the mean value of kinetic energy of electrons and, therefore, the higher the probability of tunneling of carriers through the barrier. The flux q_+ of carriers from the hot to the cold bank of the junction is larger than the reverse carrier flux q_- from the cold to the hot bank, i.e., the charge transfer through the junction takes place until a built-in potential equalizes the carrier fluxes.

Meanwhile, under certain conditions, the amount of carriers transported through the metal cross-section can depend strongly on temperature. This may take place, for example, when a metallic conductor is split into parts so that carrier tunneling between such parts is possible; see Fig. 9. Obviously, the tunneling probability depends strongly on the energy of tunnel carriers and, therefore, on the carrier temperature. Thus, under certain conditions, one can expect a considerable charge transport through the tunnel junction caused by a temperature gradient across the junction and, therefore, one can expect large α for tunnel junctions in metals.

4.1. The Model

For simplicity, we consider two equal conductors made of the same metal with flat bank borders separated by distance h (see Fig. 9). We assume that some medium fills the space between the conductor borders. The left-hand-side conductor has temperature T_1, and the right-hand-side conductor has temperature $T_0 < T_1$. Electrons from the left-hand-side conductor are tunneling to the right-hand-side one, providing a current of density j_+, and electrons tunneling back provide a current of density j_-. Since the electrons in the left-hand-side (hot) conductor have a larger thermal kinetic energy, they have a larger probability of tunneling than the electrons in the right-hand-side (cold) conductor with a lower thermal energy. Therefore, some additional amount of carriers comes from the hot conductor to the cold conductor, and a thermal built-in voltage appears between the conductors.

Let us take the potential $\varphi_1 = 0$ (electric potential is constant everywhere in the conductor) for the left-hand-side conductor and $\varphi_0 = U$ for the right-hand-side conductor. Far sides of the conductors are connected through the load, so that the thermal current j flows through the conductors. We describe the current–voltage (CV) characteristics $j(U)$ of a tunnel junction shown in Fig. 9 in the following section.

4.2. Current–Voltage Characteristics of Tunnel Junctions

Assume that banks of the junction shown in Fig. 9 build a rectangular potential barrier for carriers. For simplicity, here we restrict ourselves to a relatively simple model of tunneling. In particular, we

do not take into account multiple scattering of tunneled carriers on the conductor surfaces, in spite of the fact that such a scattering may noticeably influence the carrier transfer in experiments as was, for example, pointed out in [9].

We take the probability W of electron tunneling through a rectangular barrier of width h and height V from [15] (p. 106) as follows:

$$W(k_z) = \frac{4k_z^2\varkappa^2}{(k_z^2+\varkappa^2)^2\sinh^2(h\varkappa)+4k_z^2\varkappa^2}, \tag{17}$$

where k_z is the component of the wave vector of electron in the z-axis direction normal to the bank surfaces, $\varkappa = \hbar^{-1}\sqrt{2m(V-E_z)} \equiv \hbar^{-1}\sqrt{2m[V-\hbar^2k_z^2/(2m)]}$ with m the electron mass, $E_z = E - (\hbar^2/2m)(k_x^2+k_y^2) = \hbar^2k_z^2/(2m)$ is the part of the electron kinetic energy related to its motion along the z axis, E is the total electron kinetic energy, and k_x and k_y are components of the electron wave vector along the x and y axes. The barrier height is $V = \varepsilon_F + \chi$, where ε_F is the Fermi energy and χ is the work function for the metal of conductors.

The current density dj_+ of electrons tunneling through the barrier from a conductor with temperature T_1 to a conductor with temperature T_0 and having kinetic energy in the domain $E - E + dE$ is

$$dj_+ = \frac{e\hbar k_z}{m}W(k_z)f_{F1}(T_1,k)[1-f_{F0}(T_0,k)]dn, \tag{18}$$

where e is the electron charge (here and below $e>0$),

$$f_{F1}(T_1,k) = [1+\exp\{[(\hbar k)^2/(2m)-\varepsilon_F]/(k_BT_1)\}]^{-1}, \tag{19}$$

$$f_{F0}(T_0,k) = [1+\exp\{[(\hbar k)^2/(2m)-\varepsilon_F-eU]/(k_BT_0)\}]^{-1} \tag{20}$$

are the Fermi distribution functions, $k^2 = k_x^2+k_y^2+k_z^2$ is the square modulus of the electron wave vector, and $dn = 2(dk_x\,dk_y\,dk_z)/(2\pi)^3$ is the density of electron states with kinetic energy in the domain $E-E+dE$. The value $-eU$ in Eq. (19) is the electron potential energy related to the voltage between the metal with temperature T_1 and the metal with temperature T_0, and k_B is the Boltzmann constant. The multiplier $[1-f_{F0}(T_0,k)]$ in Eq. (18) is the relative number of free places for electrons in a conductor with temperature T_0. The current density dj_- of electrons tunneling through the barrier from the conductor with temperature T_0 to the conductor with temperature T_1 with kinetic energy of carriers in the domain $E - E + dE$ is

$$dj_- = \frac{e\hbar}{m}k_zW(k_z)f_{F0}(T_0,k)[1-f_{F1}(T_1,k)]\,dn. \tag{21}$$

The total current density j through the tunnel junction reads

$$j = \int dj_+ - \int dj_-. \tag{22}$$

The terms $\sim f_{F0}f_{F1}$ in relations (18) and (21) cancel each other in Eq. (22), so that Eq. (22) can be rewritten as follows:

$$j = \frac{e\hbar}{4\pi^3m}\int dk_x\,dk_y\,dk_z\,k_zW(k_z)[f_{F1}(T_1,k)-f_{F0}(T_0,k)]. \tag{23}$$

Since W does not depend on k_x and k_y, one can take integrals on dk_x and dk_y in Eq. (23) and arrive at

$$j(U) = \frac{ek_B}{2\pi^2\hbar}\int_0^{\sqrt{2mV}/\hbar} k_z\,dk_z\,W(k_z)[F_1(T_1,k_z) - F_0(T_0,k_z,U)], \tag{24}$$

where

$$F_1(T_1,k_z) = T_1\ln\left[\frac{1+\exp\{[\varepsilon_F - (\hbar k_z)^2/(2m)]/(k_BT_1)\}}{1+\exp[\chi/(k_BT_1)]}\right],$$
$$F_0(T_0,k_z,U) = T_0\ln\left[\frac{1+\exp\{[\varepsilon_F + eU - (\hbar k_z)^2/(2m)]/(k_BT_0)\}}{1+\exp[\chi/(k_BT_0)]}\right].$$

In view of the notation $z = [(\hbar k_z)^2/(2m) - \varepsilon_F]/e$, one can reduce Eq. (24) to

$$j(U) = \frac{me^2k_B}{2\pi^2\hbar^3}\int_{-\bar\varepsilon_F}^{\bar\chi} dz\bar W(z)\left[\bar F_1(T_1,z) - \bar F_0(T_0,z,U)\right], \tag{25}$$

where $\bar\varepsilon_F = \varepsilon_F/e$ and $\bar\chi = \chi/e$ are, respectively, the Fermi energy and the work function in [eV],

$$\bar F_1(T_1,z) = T_1\ln\left\{\frac{1+\exp[-z/(\xi T_1)]}{1+\exp[\bar\chi/(\xi T_1)]}\right\},$$
$$\bar F_0(T_0,z,U) = T_0\ln\left\{\frac{1+\exp[(-z+U)/(\xi T_0)]}{1+\exp[\bar\chi/(\xi T_0)]}\right\}, \qquad \xi = k_B/e, \tag{26}$$

$$\bar W(z) = \frac{4(\bar\chi - z)(\bar\varepsilon_F + z)}{(\bar\varepsilon_F + \bar\chi)^2\sinh^2\left[(\sqrt{2me}h/\hbar)\sqrt{\bar\chi - z}\right] + 4(\bar\chi - z)(\bar\varepsilon_F + z)}. \tag{27}$$

Equation (25) can be simplified.

Under the usual conditions, one can expect $U \ll z$ and $T_1 - T_0 \ll T_0$. Then $\bar F_0(T_0,z,U)$ can be presented as a series over U and the difference $\bar F_1(T_1,z) - \bar F_0(T_0,z,U=0)$ as a series over $T_1 - T_0$; in both cases we keep first-order terms and neglect higher-order terms. After some algebra, we arrive at the following approximate relation instead of Eq. (25):

$$j(U) = j_T(T_0)(T_1 - T_0) - \sigma(T_0)U, \tag{28}$$

where $j_T(T_0)(T_1 - T_0)$ is the short-cut (i.e., at $U = 0$) current density. Equation (25) reads

$$j_T(T_0) = \frac{\sigma_0}{T_0}I_j(T_0), \qquad \sigma_0 = \frac{me^3}{2\pi^2\hbar^3} = 1.612\cdot 10^{14}\ [\mathrm{A\cdot V}]^{-1}, \tag{29}$$

with

$$I_j(T_0) = \int_{-\bar\varepsilon_F}^{\bar\chi} dz\,\bar W(z)\left\{\xi T_0\ln\left[\frac{1+e^{-z/(\xi T_0)}}{1+e^{\bar\chi/(\xi T_0)}}\right] + \frac{z}{1+e^{z/(\xi T_0)}} + \frac{\bar\chi}{1+e^{-\bar\chi/(\xi T_0)}}\right\}.$$

The conduction $\sigma(T_0)$ of a tunnel junction of unit area is

$$\sigma(T_0) = \sigma_0 I_\sigma(T_0), \qquad I_\sigma(T_0) = \int_{-\bar\varepsilon_F}^{\bar\chi}\frac{\bar W(z)\,dz}{1+\exp(z/\xi T_0)}. \tag{30}$$

The linear current–voltage relation (28), where j_T and σ are given by (29) and (30), is the basic relation for the analysis presented below.

4.3. Thermo-EMF Coefficient and Figure of Merit for Tunnel Junctions

At a current $j = 0$ through a junction, there exists a "free running" voltage $U \equiv U_0$ at the junction. One can find U_0 by solving the equation that follows from Eq. (25),

$$\int_{-\bar{\varepsilon}_F}^{\bar{\chi}} dz\, \bar{W}(z) \left[\bar{F}_1(T_1, z) - \bar{F}_0(T_0, z, U_0)\right] = 0, \tag{31}$$

or taking

$$U_0 = j_T(T_1 - T_0)/\sigma = \left(\frac{T_1}{T_0} - 1\right) U_*(T_0), \qquad U_*(T_0) = \frac{I_j(T_0)}{I_\sigma(T_0)} \tag{32}$$

from (28). Then the thermo-EMF coefficient $\alpha = U_0/(T_1 - T_0)$ is

$$\alpha(T_0) = \frac{U_*(T_0)}{T_0}\,. \tag{33}$$

Figure 10 shows the dependence $\alpha(h)$ for the tunnel junction of Cu conductors with $\varepsilon_F = 7$ eV for three different temperatures $T_0 = 400$, 500, and 600 K. We assume the presence of some medium inside the tunnel junction in Fig. 9 such that the work function for electrons in Cu is smaller than the work function 4.4 eV for the transition from Cu to vacuum. For definiteness, we take $\chi = 2$ eV. The search for proper media to fill the junction and developing the technology for constructing the tunnel junction shown in Fig. 9 are out of the scope of the present paper. When the proper material for filling the junction is found, the junction can be manufactured by many methods of thin-layer depositions such as, for example, chemical deposition or magnetron deposition [16].

In Fig. 10, one can see that, for chosen values of the parameters, the α for the tunnel junction of Cu conductors is of the order of several hundreds of μV/K, which is even larger than typical values of α for semiconductors $\alpha{\sim}150$ μV/K [10] (p. 308); otherwise, one can see the $\alpha(h)$ maxima.

The dependences in Fig. 10 are found from approximate relation (33); nevertheless, they fit very well the ones found from numerical solution of Eq. (31). This means that the current–voltage characteristics of the tunnel junction with the given parameters are linear, and the optimum working point of the junction (i.e., the maximum output power) corresponds to the voltage across the junction $U = U_0/2$ and, correspondingly, the current through the junction is $j_T(T_1 - T_0)/2$, and the load resistance must be the same as the junction resistance.

In order to estimate the figure of merit of the tunnel junction, one must know the coefficient $\varkappa_j$ of the heat conductance and the specific resistance ϱ_j of the junction. They depend on the tunnel current, specific resistance, and heat conduction of the medium between the junction banks.

First, we assume that the medium between the banks is a metal or heavily doped semiconductor, and that $\varkappa_j$ and ϱ_j are related by the Wiedemann–Franz law, so that $\varkappa_j \varrho_j = LT$. Figure 11 shows the figure of merit $\alpha^2/(4L)$ [see Eq. (13)] for this case, where α is determined by Eq. (33).

Comparing Figs. 11 and 7, one can see that the figure of merit of the tunnel junction is one to two orders of magnitude greater than the figure of merit of a well-known metal thermocouple. Similar to $\alpha(h)$, the dependence of the figure of merit on h has a maximum.

Another way to estimate the Q-factor of the tunnel junction is to assume that the thermal flux and current through the junction are determined by the tunnel carriers. In this case, we take the specific resistance as follows:

$$\varrho_j = [\sigma(T_0)h]^{-1}, \tag{34}$$

where $\sigma(T_0)$ is given by Eq. (30), and calculate the thermal flux through the tunnel junction

$$q(T_1, T_0, U) = \frac{\hbar^3}{8\pi^3 m^2} \int dk_x\, dk_y\, dk_z\, k^2 k_z W(k_z)[f_{F1}(T_1, k) - f_{F0}(T_0, k, U)]. \tag{35}$$

Then, expanding Eq. (35) in series over $(T_1 - T_0)$ and over U and taking U at the working point $U = U_0/2$, where U_0 is given by Eq. (32), we calculate the heat conduction coefficient

$$\varkappa_j(h, T_0) = \lim_{T_1 \to T_0} [q(T_1, T_0, U_0/2)h/(T_1 - T_0)]$$

as follows:

$$\varkappa_j(h, T) = \frac{\hbar^3 h}{8\pi^3 m^2} \int dk_x\, dk_y\, dk_z\, k^2 k_z W(k_z) \left[\frac{\partial f_{F1}(T, k)}{\partial T} - \frac{\alpha(T)}{2} \left. \frac{\partial f_{F0}(T, k, U)}{\partial U} \right|_{U=0} \right]. \tag{36}$$

The figure of merit of the tunnel junction $ZT = \alpha^2/(\varrho_j \varkappa_j)$ with ϱ_j and $\varkappa_j$ given, respectively, by Eqs. (34) and (36) is shown in Fig. 12.

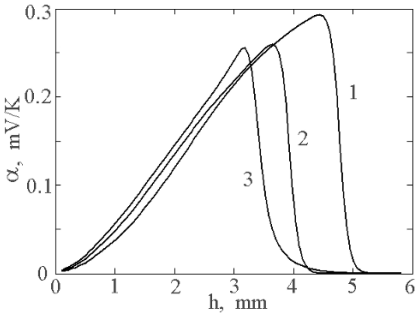

Fig. 10. Thermo-EMF coefficient of Cu versus the tunnel-junction width for three different temperatures 400 K (1), 500 K (2), and 600 K (3).

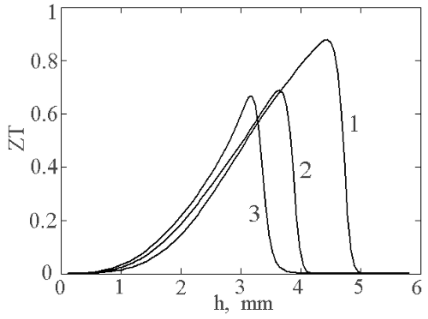

Fig. 11. Figure of merit of the tunnel junction for three different temperatures 400 K (1), 500 K (2), and 600 K (3) calculated using the Wiedemann–Franz law.

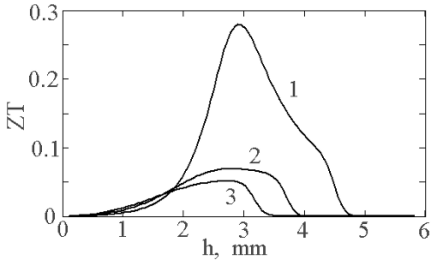

Fig. 12. Figure of merit of the tunnel junction for three different temperatures 400 K (1), 500 K (2)m and 600 K (3) obtained by calculations of $\varkappa_j$ and ϱ_j using Eqs. (34) and (36).

From Figs. 11 and 12, one can see that the approach where the figure of merit is calculated using Eqs. (34) and (36) gives a lower Q-factor than that calculated in view of the Wiedemann–Franz law, but is still several times or even one order of magnitude greater than the Q-factor in Fig. 7 for a Fe–constantan thermocouple. In both cases in Figs. 11 and 12, the figure of merit has a maximum at a certain width h of the tunnel junction, and it is greater at lower than at higher temperatures.

5. Conclusions

Our estimates show that the thermo-EMF coefficient of the tunnel junction in metals can reach hundreds of μV/K, which is even larger than the thermo-EMF coefficient of semiconductor thermoelements. The large α leads to a large figure of merit ZT that is several times or even one to two orders of magnitude greater (approaching $ZT \to 1$) than the figure of merit for metal thermocouples. This explains the

necessity of studying materials with tunnel junctions, in particular, metals as prospective thermoelectric materials. Meanwhile, there is a large field for theoretical and experimental studies of thermoelectrics with tunnel junctions. In particular, one has to find optimum parameters of junctions, such as the width and height of the barriers providing the maximum of the figure of merit with more precise description of heat conduction through the junction. One has to choose properly and describe in detail the medium between the junction banks and the shape of the barrier taking into account the carrier diffusion and built-in voltage.

In this paper, we restricted ourselves to a junction with metal banks. However, it may be interesting to consider tunnel junctions in semiconductor materials and compare the results for such materials with that obtained in the case of p–n junctions in semiconductors in [7].

In future theoretical studies, one needs to take into account in detail the carrier scattering on junction banks, which may lead to additional noise in thermal power and even change the thermal-power sign [9]. It may be interesting to carry out experimental studies of thermoelectric power on tunnel junctions using atomic force microscope in a tunnel mode. In order to provide a large change in the temperature and sufficient output voltage, one needs to connect in series many tunnel junctions, making a thin multilayer TEG. There exists considerable interest in thin layer TEGs at present; see, for example, [17]. One can expect that the construction and technology of manufacturing thin-layer TEGs with tunnel junctions will be simpler than the construction and technology of thin-layer semiconductor TEGs, using traditional Stonehenge design as, for example, in [18].

References

1. *Thermoelectric Generators. General Information.* [http://newenergetika.narod.ru/termoerektrogeneratory/termoerektrogeneratory.html].
2. A. Belevtsev, V. Bogatov, A. Karzhavin, et al., "Thermoelectric temperature converters: practice, evolution," *CTA*, **2**, 66 (2004) [http://www.cta.ru/english/issues/239852.htm].
3. N. V. Kolomoets, *Thermoelectric Generator*, in: Encyclopedia of Physics [in Russian], Great Russian Encyclopedia Publishers, Moscow (1998), Vol. 5, p. 99.
4. A. F. Ioffe, "About increase in the efficiency of semiconductor thermocouples," *Selected Papers* [in Russian], Nauka, Leningrad (1975), Vol. 2, p. 313.
5. G. D. Alekseeva, "Heat conductance of halcogenides of Pb and solid solutions based on PbTe," PhD Thesis, RGB OD 61:85-1/1122 [http://www.lib.ua-ru.net/diss/cont/188475.html].
6. I. Tautz, *Photo and Thermoelectric Phenomena in Semiconductors*, Inostrannaya Literatura, Moscow (1962).
7. Yu. I. Ravich and D. A. Pshenay-Severin, *Semiconductors (Fiz. Tekh. Poluprovodn.)*, **35**, 1214 (2001).
8. A. Glatz and I. S. Beloborodov, *Phys. Rev. B*, **79**, 235403 (2009).
9. B. Ludoph and J. M. van Ruitenbeek, *Phys. Rev. B*, **59**, 12290 (1999).
10. A. F. Ioffe, "Energy background of thermoelectric semiconductor batteries," *Selected Papers* [in Russian], Nauka, Leningrad (1975), Vol. 2, p. 271.
11. L. D. Landau and E. M. Lifshitz, *Electrodynamics of Continuous Media* [in Russian], Fizmatlit, Moscow (2001), p. 154.
12. E. M. Epshtein, "Wiedemann–Franz law," in: *Encyclopedia of Physics* [in Russian], Sovet Encyclopedia Publishers, Moscow (1988), Vol. 1, p. 275.

13. L. S. Stilbans, "Thermo-EMF," in: *Encyclopedia of Physics* [in Russian], Great Russian Encyclopedia Publishers, Moscow (1998), Vol. 5, p. 97.
14. I. S. Grigoriev and E. Z. Meilikhov (eds.), *Physical Quantities. Handbook*, Energoatomizdat, Moscow (1991).
15. L. D. Landau and E. M. Lifshitz, *Quantum Mechanics*, Nauka, Moscow (1989).
16. E. Berlin and L. Seydman, *Electronics: Sci., Technol., Business*, **2**, 88 (2006).
17. J. H. Kiely and Dong-Hi Leez, *Measur. Sci. Technol.*, **8**, 661 (1997).
18. T. Schneider, R. Alley, D. Koester, and S. Lee, "Thin film thermoelectric power generation," Nextreme Thermal Solutions (May 3, 2007) [http://www.nextreme.com/media/pdf/whitepapers/Nextreme_Thin_Film.pdf].